FULL PAPER

Chitosan–Alginate Microcapsules Provide Gastric Protection and Intestinal Release of ICAM-1-Targeting Nanocarriers, Enabling GI Targeting In Vivo

Rasa Ghaffarian, Edgar Pérez-Herrero, Hyuntaek Oh, Srinivasa R. Raghavan, and Silvia Muro*

When administered intravenously, active targeting of drug nanocarriers (NCs) improves biodistribution and endocytosis. Targeting may also improve NC oral delivery to treat gastrointestinal (GI) pathologies or for systemic absorption. However, GI instability of targeting moieties compromises this strategy. This study explores whether encapsulation of antibody-coated NCs in microcapsules would protect against gastric degradation, providing NC release and targeting in intestinal conditions. Nanoparticles coated with antibodies against intercellular adhesion molecule-1 (anti-ICAM) or nonspecific immunoglobulin G (IgG) are encapsulated in chitosan (shell) - alginate (core) microcapsules. Encapsulation efficiency is >95% and NC relase from microcapsules in storage is <10%. There is minimal NC release at gastric pH (<10%) and burst release at intestinal pH (75%–85%). Encapsulated NCs afford increased protection against degradation (threefold to fourfold) and increased cell targeting (8–20-fold) after release versus the nonencapsulated NCs. Mouse oral gavage shows that microencapsulation provides 38%–65% greater protection of anti-ICAM NCs in the GI tract, 40% lower gastric retention, and fourfold to ninefold enhanced intestinal biodistribution versus nonencapsulated NCs. Therefore, microencapsulation of antibody-targeted NCs may enable active targeting strategies to be effective in the context of oral drug delivery.

1. Introduction

Active targeting of therapeutics to specific markers within the body enhances biodistribution to disease sites, minimizing

Dr. R. Ghaffarian, Prof. S. Muro
Fischell Department of Bioengineering
2330 Jeong H. Kim Engineering Building
University of Maryland
College Park, MD 20742, USA
E-mail: muro@umd.edu
Dr. E. Pérez-Herrero, Prof. S. Muro
Institute for Bioscience and Biotechnology Research
5115 Plant Sciences Building
University of Maryland
College Park, MD 20742, USA
Dr. H. Oh, Prof. S. R. Raghavan
Department of Chemical and Biomolecular Engineering
1227C Chemical & Nuclear Engineering Building
University of Maryland
College Park, MD 20742, USA

toxicity.[1–3] Targeting involves coupling of drugs to affinity biomolecules, such as vitamins, peptides, antibodies, aptamers, etc., enabling binding to markers expressed on the target cells.[1–3] Targeting moieties can also be coupled onto drug nanocarriers (NCs) used to improve drug solubility, stability, metabolism, and clearance.[3,4]

In addition to improving drug biodistribution toward selected cells, active targeting is also used to trigger receptor-mediated endocytosis.[2,3] In this process, the ligand–receptor complex is engulfed within endocytic vesicles that carry the ligand intracellularly.[2,3] Endocytic vesicles can also traffic across the cell body with release at the basolateral side via transcytosis.[1–3] This allows for transport across cells that control the passage of substances between body compartments, e.g., the endothelial lining that separates the bloodstream from underlying tissue or epithelial barriers at other interfaces.[1–3]

In the context of oral drug delivery, active binding and/or uptake by gastrointestinal (GI) epithelial cells may improve treatment of GI disorders, while transport across this lining may enhance absorption into the circulation.[5,6] Indeed, mucosal adhesion and absorption has been enhanced by targeting vitamin, carbohydrate, and integrin receptors on the GI epithelium.[6–11] However, this strategy is limited by deactivation of targeting molecules in the acidic and hydrolytic environment of the stomach, which curtails intestinal targeting.[12] There is a need for protection of drug carriers from degradation in gastric conditions and release in intestinal conditions, while preserving the activity of their targeting moieties.

As an example, this study seeks to improve GI targeting of NCs addressed to intercellular adhesion molecule-1 (ICAM-1), a glycoprotein expressed on various cell types and upregulated in many pathological conditions, including GI epithelium.[13,14] ICAM-1 targeting induces transport into and across cells via a clathrin- and caveolae-independent pathway,[15–19] enhancing delivery of therapeutics into and across GI epithelial monolayers in culture.[18] Implementation of this strategy via oral gavage in mice has shown promise, as specific targeting was observed versus nontargeted NCs.[20] Yet, intestinal

biodistribution was restricted by NC retention in the stomach, with substantial degradation.[20] Therefore, anti-ICAM NCs and other targeted formulations could benefit from protection and site-specific release in the GI tract.

Many strategies have been used to encapsulate oral drugs and enhance their protection from low gastric pH and enzymatic hydrolysis, and to provide release in intestinal conditions.[21] Among the most commonly used polymers for this purpose is alginate, a naturally occurring, anionic polysaccharide that is inexpensive, biocompatible, and biodegradable.[22–24] Dropwise addition of alginate to an aqueous crosslinking solution of divalent cations (e.g., Ca^{2+}) results in the formation of gel-like particles.[22–28] Alginate has been widely used for encapsulation of biological agents, such as microbial and eukaryotic cells, proteins, antibodies, vaccines, etc.[22–32] These capsules are often reinforced with a chitosan shell during or after alginate-particle formation.[22] Chitosan is a natural, cationic polysaccharide that forms spontaneous electrostatic complexes with alginate.[22] Chitosan–alginate capsules show greater mechanical stability, and reduced drug leaching and burst release compared to alginate alone.[22,33] Chitosan is also mucoadhesive, which prolongs residence time in the intestine.[22,32–36] To our knowledge, encapsulation of targeted (antibody-coated) NCs in chitosan–alginate microcapsules for oral delivery is yet to be examined. Using the example of ICAM-1-targeting NCs, this study aimed at exploring the said strategy.

2. Results

2.1. Preparation of Antibody-Coated NCs

To improve GI targeting by anti-ICAM NCs in vivo, we aimed at encapsulating the NCs within microcapsules to protect their labile targeting moiety from premature gastric degradation. As an NC model, we used polystyrene nanoparticles labeled with a pH-independent fluorophore and coated by surface adsorption with nonspecific immunoglobulin G (IgG) or anti-ICAM. Since polystyrene is not biodegradable, this allows us to examine the antibody counterpart in GI conditions (our focus) without confounding effects of polymer degradation. This model displays similar ICAM-1 binding, endocytosis, and in vivo biodistribution as NCs of biocompatible poly(lactic-co-glycolic acid).[37,38] Surface adsorption of antibodies on particles preferentially renders outward display of variable regions at the used concentrations.[39] A random orientation is also possible, similar to random covalent conjugation of antibodies where the conjugation occurs at any of the available antibody residues. Extensive characterization of our formulation has shown negligible coating with serum albumin (presumably due to saturation of the NC surface with antibodies), without apparent changes in fluorescence intensity, nor aggregation or antibody detachment.[15–20,37,38,40–45] The antibody coating, hydrodynamic size, polydispersity index, and ζ-potential were highly reproducible.[15–20,37,38,40–45] Implementation of this protocol rendered similar characteristics for IgG NCs and anti-ICAM NCs: the hydrodynamic diameter was 158 ± 5 nm and 156 ± 2 nm, the polydispersity was 0.19 ± 0.03 and 0.22 ± 0.05, the ζ-potential was −31 ± 2 mV and −27 ± 5 mV, and the coat

contained 176 ± 8 IgG molecules per NC and 208 ± 43 anti-ICAM molecules per NC. For cellular targeting and in vivo oral gavage in mice, we used anti-ICAM NCs compared to nonspecific IgG NCs. For in vitro assays where encapsulation, protection, and release (not targeting) were the focus, we used IgG NCs since IgG is less costly and has similar molecular characteristics to anti-ICAM.

2.2. Preparation of NC-Loaded Alginate and Chitosan–Alginate Microcapsules

Whereas biopolymers have been extensively studied for encapsulation of biological and pharmaceutical agents, and to a lesser extent for encapsulation of nontargeted NCs,[25–33,46] microencapsulation of antibody-coated NCs within these materials had not yet been assessed. We selected alginate based on its biocompatibility and gentle formulation.[22,23] Encapsulation was achieved by mixing ^{125}I-antibody-coated fluorescent NCs with a solution of sodium alginate and by then generating droplets using a described co-axial air flow technique,[47] whereby collection of the droplets in a crosslinking solution of $CaCl_2$ rendered microcapsules (**Figure 1**A). We compared these alginate microcapsules to formulations where subsequent incubation with 0.25% chitosan rendered a chitosan shell around the alginate microcapsules, which may help minimize changes in size and loading (Figure 1B). Both preparations rendered monodisperse spherical capsules with a diameter ≈180 μm, as observed by phase contrast and fluorescence microscopy (Figure 1F and **Figure 2**A). Fluorescence visualization also confirmed the presence of a chitosan shell (red) for the corresponding microcapsules, and NCs (green) distributed within the alginate core (Figure 2B). Fluorescence quantification revealed similar loading in both formulations (≈1.2 × 10⁸ arbitrary units, A.U.; Figure 2C), corresponding to ≈1.9 × 10⁶ NCs per microcapsule, as quantified by radiotracing the antibody counterpart (Figures 1F and 2C). As such, % loading and encapsulation efficiency (EE%) were similar for both alginate and chitosan–alginate microcapsules (≈15% loading and ≈98 EE%; Figure 1F). Therefore, formulations had similar physical and loading characteristics irrespective of the chitosan shell, and both radioisotope and fluorescence tracing are viable methods to examine these parameters.

2.3. Stability of NC-Loaded Microcapsules in Storage Conditions

To assess the stability of these formulations in storage conditions (2% $CaCl_2$ at 4 °C for 28 d), we first examined the release of ^{125}I-IgG-coated fluorescent NCs from the microcapsules over time. Both radioisotope tracing of the antibody coat (**Figure 3**A) and spectrofluorometry of the NC counterpart (Figure S1A, Supporting Information) revealed minimal release (<10%) from either alginate or 0.25% chitosan–alginate over 28 d, indicating microcapsule stability. Similar release found by tracing the antibody or NC counterparts also suggest the stability of antibody-coated NCs within the microcapsule. Supporting this, when microcapsules were dissolved by incubation with Ethylenediaminetetraacetic acid (EDTA), the released NCs bound to
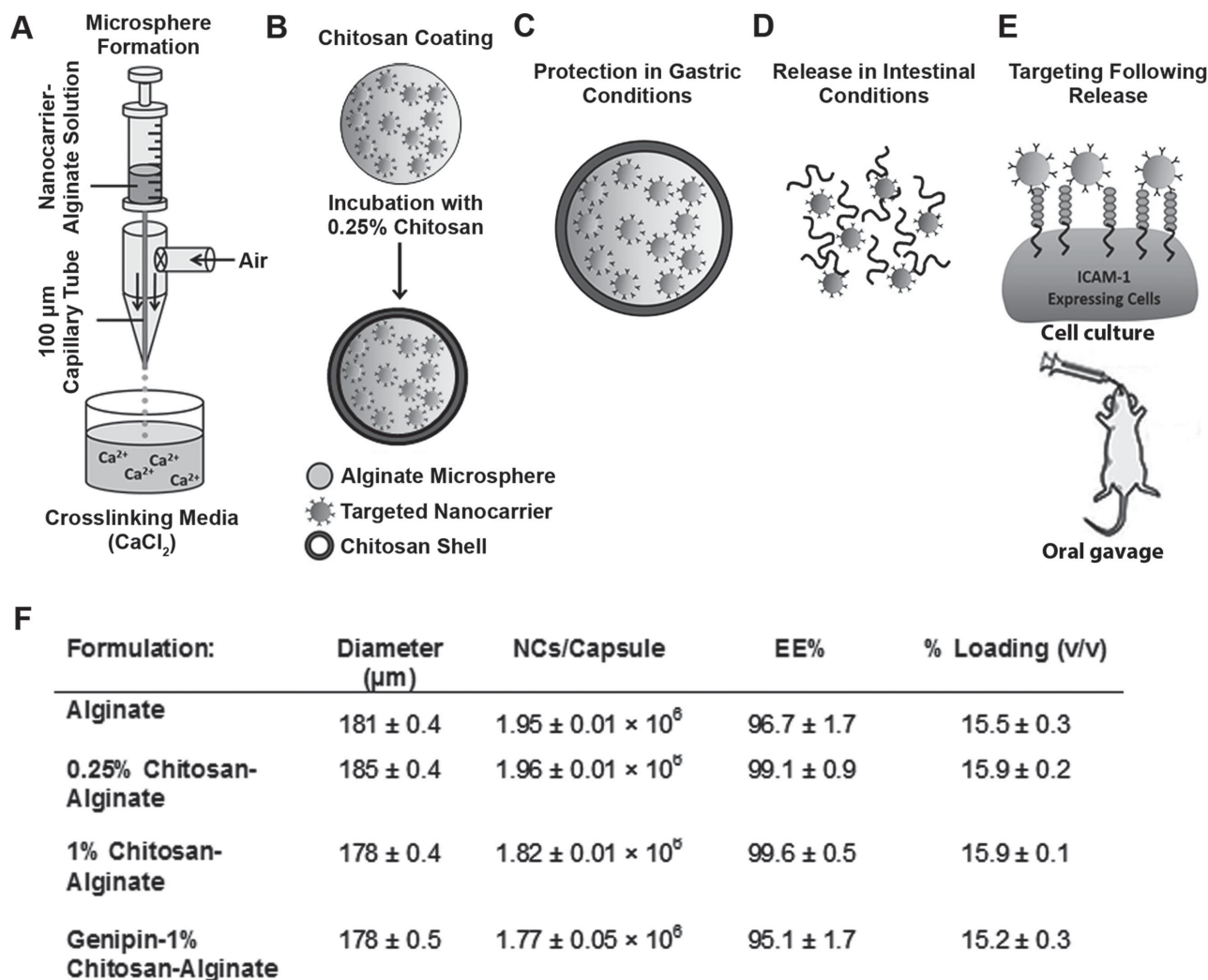
Figure 1. Scheme of the method and intended goal, and microcapsule characterization. A) Encapsulation of ICAM-1-targeting nanocarriers (anti-ICAM NCs) in alginate (core) microcapsules, B) which are then coated with a chitosan shell. C) These microcapsules provide protection against gastric degradation and D) release in intestinal conditions, E) enabling NCs to target ICAM-1 of GI cells and the GI in mice. F) Characterization of microcapsules loaded with antibody-coated NCs.

a surface-immobilized target with ≈90% the efficiency of antibody-coated NCs that had never been encapsulated (Figure 3B). In agreement, only minimal amounts of free ^{125}Iodine (<5%; Figure 3C), indicative of antibody degradation, were found upon dissolving microcapsules with EDTA. The size, number, and fluorescence content of alginate or chitosan–alginate microcapsules, measured by fluorescence microscopy, did not differ between the two formulations nor decreased over 28 d in storage (Figure 3D; Figure S1B, Supporting Information). Hence, encapsulated antibody-coated NCs are not degraded and retain their binding capacity during encapsulation and storage, concurrent with microcapsule stability.

2.4. pH-Dependent Release of Antibody-Coated NCs from Microcapsules

Next, we examined whether microencapsulation provided the intended release pattern at intestinal pH, while precluding premature release at gastric pH. Alginate and 0.25% chitosan–alginate microcapsules were incubated in simulated gastric fluid (SGF) (pH 1.2) for 2 h, followed by simulated intestinal fluid (SIF) (pH 7.8) for 4 h. These experiments were conducted without GI enzymes to assess the effect of pH transitions on release, while subsequent experiments examined microcapsule behavior in the presence of GI enzymes. As per radioisotope tracing (**Figure 4**A), microcapsules exhibited negligible NC release in SGF, with a slightly lower (not significant) release in the presence of the chitosan shell (1% vs 5% for alginate alone). Accordingly, the number of visible microcapsules, their size, and their fluorescence content did not vary much in gastric pH: ≈85%–95% of microcapsules appeared intact (Figure 4B), their size was only reduced by ≈20%–30% (Figure 4C), and they retained ≈95% of the initial sum fluorescence content while the mean fluorescence per area increased ≈40% (Figure S2, Supporting Information). This suggests that in gastric pH, microcapsules shrank to a

www.MaterialsViews.com

ADVANCED
FUNCTIONAL
MATERIALS
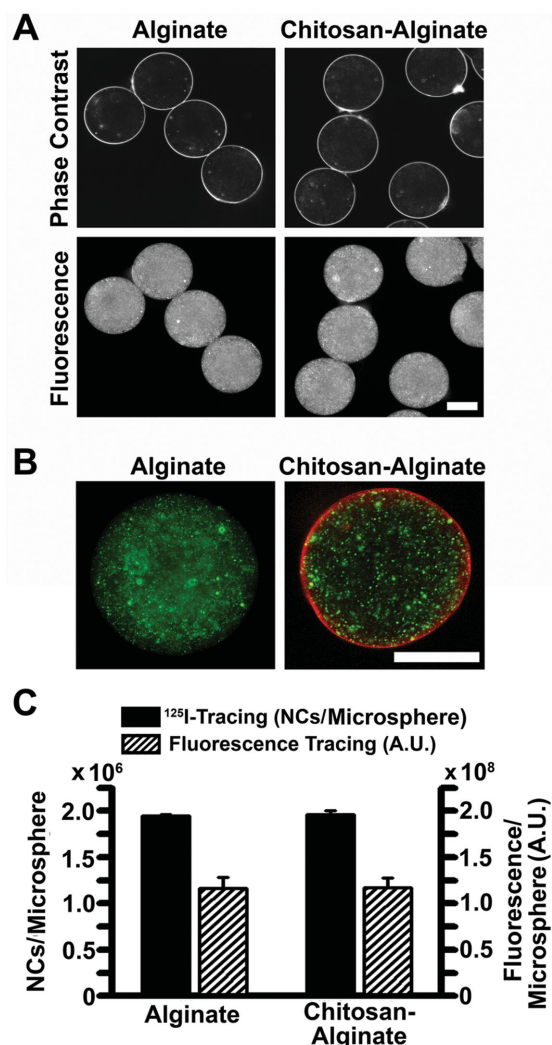www.afm-journal.de

FULL PAPER

Figure 2. Encapsulation of antibody-coated NCs into alginate or chitosan–alginate microcapsules. ^{125}I-IgG-coated, fluorescent NCs were encapsulated into alginate microcapsules with or without a chitosan shell. A) Phase contrast and fluorescence microscopy images of both types of microcapsules. B) Dual-fluorescence visualization of microcapsules, with green NCs within the alginate core, in the presence (right) or absence (left) of a red rhodamine-labeled chitosan coat. (A,B) Scale bar = 100 μm. C) Loading assessed by radioisotope quantification of the antibody coat or fluorescence (A.U.) of the NC counterpart. Data are Mean ± S.E.M. No statistically significant differences between alginate and chitosan–alginate formulations were observed.

modest degree, yet did not release NCs and may, hence, protect NCs in this environment.

Upon transferring microcapsules to SIF, both formulations displayed burst release of antibody-coated NCs within the first hour (60%–75% release), albeit to a lower extent for chitosan-coated microcapsules (20% lower release; Figure 4A). Alginate microcapsules reached maximum release by this time, while release from chitosan–alginate microcapsules reached a plateau 4 h after transfer to SIF (Figure 4A). Therefore, the chitosan shell may help modulate release, as expected. In agreement, alginate microcapsules fully dissolved by 4 h in SIF (Figure 4B,C) and no fluorescent content could be measured
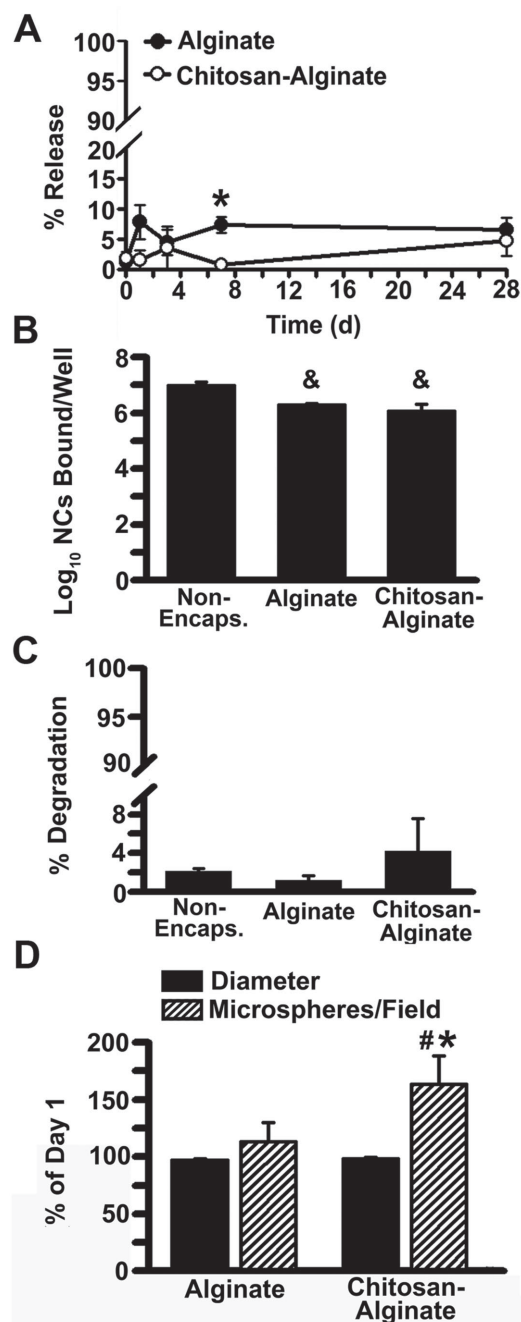

Figure 3. Stability of NC-loaded microcapsules in storage conditions. Alginate versus 0.25% chitosan–alginate microcapsules loaded with ^{125}I-IgG-coated fluorescent NCs were incubated in CaCl₂, at 4 °C. A) At the indicated times, the radioisotope content of the released and encapsulated fractions were measured. B) After 24 h in storage, the encapsulated ^{125}I-IgG-coated NCs were extracted from microcapsules using EDTA and their binding to surface-immobilized secondary antibody was assessed by radiotracing. C) The percentage of free [125]Iodine, indicating antibody degradation, was also evaluated. (B,C) Nonencapsulated (non-Encaps.) NCs were controls. D) After 28 d in storage, the diameter and number of microcapsules per microscopy field were analyzed from fluorescence images, and expressed as the percentage of day 1. Data are Mean ± S.E.M. * Compares alginate vs chitosan–alginate; & compares encapsulated vs nonencapsulated NCs; # compares day 28 versus day 1 (p < 0.05, Student's t test).
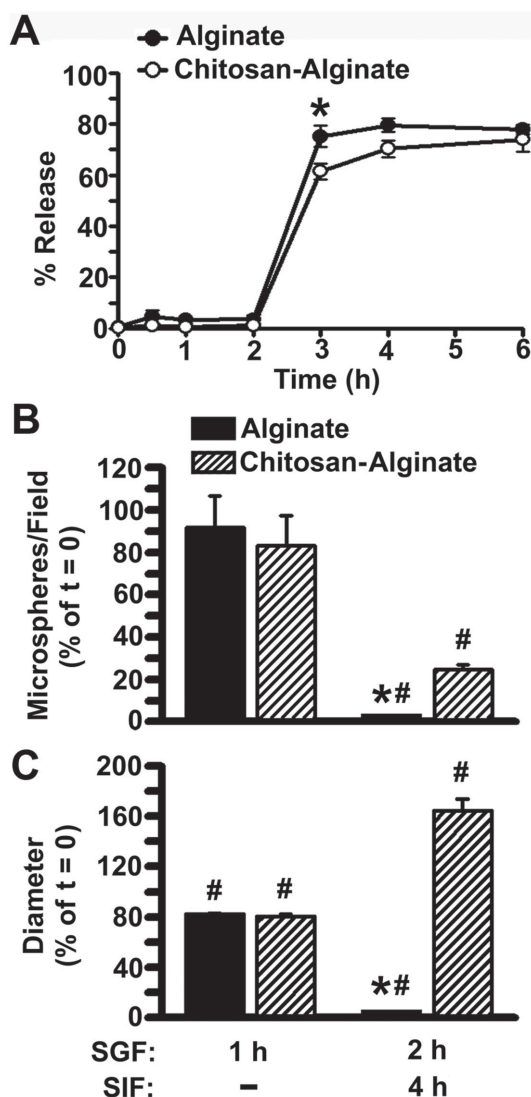
ADVANCED
FUNCTIONAL
MATERIALS
www.afm-journal.de

Materials
Views
www.MaterialsViews.com

Figure 4. pH-dependent release of NCs from microcapsules. Alginate and 0.25% chitosan–alginate microcapsules loaded with ^{125}I-IgG fluorescent NCs were incubated for 2 h at 37 °C in SGF at pH 1.2, then transferred for 4 h to SIF at pH 7.8. A) At the indicated times, aliquots were removed to assess the release of encapsulated NCs using radioisotope tracing. Aliquots were also removed after 1 h in SGF and 4 h in SIF (total incubation = 6 h) to quantify: B) the number and C) the diameter of visible microcapsules using fluorescence microscopy, expressed as the percentage of values measured prior to GI incubations ($t = 0$). Data are Mean ± S.E.M. * Compares alginate versus chitosan–alginate formulations; # compares each time point versus $t = 0$ ($p < 0.05$, Student's t test).

(Figure S2, Supporting Information). Meanwhile, 25% of the initial amount of chitosan–alginate microcapsules remained by this time (Figure 4B), which swelled to ≈160% of their initial size (Figure 4C) and retained only 50% of their initial fluorescence content (Figure S2A, Supporting Information). As a result, the mean fluorescence per area of chitosan–alginate microcapsules decreased (by 86%; Figure S2B, Supporting Information). Hence, both microcapsules showed release at intestinal but not gastric pH, and chitosan-coated formulations may help control release in this environment.

2.5. Effect of Chitosan Concentration and Crosslinking on Microcapsule Release

We then evaluated the effects of increasing the concentration of the chitosan from 0.25% to 1%, and that of crosslinking this shell with 1 mg mL^{-1} genipin, a natural aglycone that crosslinks chitosan amine groups without toxic effects of other reagents, such as glutaraldehyde.[36,48] These microcapsules had size (≈180 μm), encapsulation efficiency (≈95%), and loading capacity (≈15% w/w NCs/alginate; ≈1.8 × 10^6 NCs/bead) comparable to previous formulations (Figure 1F). Similarly negligible release of antibody-coated NCs (<4%) was observed for all formulations in SGF at pH 1.2 (**Figure 5**A), with no changes in the number of microcapsules (Figure 5B) or their fluorescence content (Figure S3A, Supporting Information). All formulations experienced a comparable shrink in SGF (≈20%; Figure 5C), hence the increased mean fluorescence per area (≈30%–50%; Figure S3A, Supporting Information).

Upon incubation in SIF at pH 7.8, microcapsules formed using 1% chitosan had similar release as 0.25% chitosan–alginate microcapsules, with 61% release by 1 h and 69% release after 4 h in SIF (Figure 5A). In agreement with radiotracing data, microscopy showed similar dissolution in SIF for both microcapsules (Figure 5B), with swelling (Figure 5C) and reduction of fluorescent content (Figure S3, Supporting Information). By 4 h, 1% chitosan–alginate microcapsules were less swelled vs 0.25% chitosan–alginate counterparts (113% vs 164% the diameter of $t = 0$; Figure 5C); hence, chitosan concentration alters morphological behavior of the microcapsules. Genipin crosslinking curtailed release by 25% after 1 h and 11% after 2 h following transfer to SIF (Figure 5A). The genipin-treated 1% chitosan–alginate formulation also swelled in SIF (Figure 5C) but retained NCs better than its uncrosslinked counterpart (Figure S3A, Supporting Information), indicating potential to modulate release.

Importantly, a similar profile of intestinal (not gastric) release was found for antibody-coated poly(D,L-lactide co-glycolide) PLGA NCs as compared to these model polystyrene counterparts (Figure S4 in the Supporting Information; 1% chitosan–alginate capsules were used as an example).

2.6. Microcapsule Protection and Release of NCs in GI Conditions

We next examined the status of ^{125}I-IgG NCs (only the antibody is labile) in the presence of gastric enzymes, to infer the protection provided by encapsulation within microcapsules. NC-loaded microcapsules versus control nonencapsulated NCs were incubated for 2 h in SGF in the presence versus absence of pepsin (**Figure 6**A). After this incubation, microcapsules were dissolved with EDTA to examine the encapsulated NCs. The level of free ^{125}Iodine (indicative of antibody degradation) indicated <10% degradation in all formulations incubated in the absence of pepsin (Figure 6A). This was expected since low pH should not result in antibody proteolysis. Most importantly, in the presence of pepsin nonencapsulated IgG NCs experienced high degree of degradation (≈70%), but this was largely attenuated by encapsulation within all microcapsule
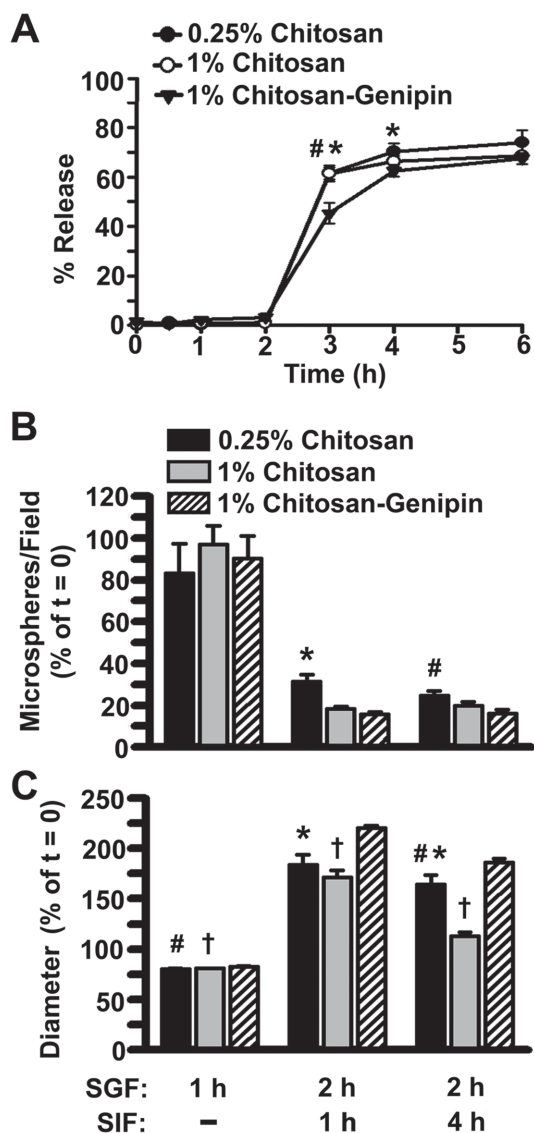
Figure 5. Effect of chitosan concentration and crosslinking on pH-dependent release from microcapsules. Alginate microcapsules containing ^{125}I-IgG fluorescent NCs were covered with a shell of either 0.25%, 1%, or genipin-crosslinked 1% chitosan, and incubated for 2 h in SGF at pH 1.2 followed by 4 h incubation in SIF at pH 7.8 (total incubation = 6 h). A) NCs released from microcapsules were assessed by radioisotope tracing of the released and encapsulated fractions, expressed a percentage of the total radioisotope content. In parallel, the B) number and C) diameter of visibly intact microcapsules were quantified from fluorescence microscopy images, and expressed as the percentage of values measured prior to incubations ($t = 0$). Data are Mean ± S.E.M. * Compares 0.25% versus 1% chitosan formulations; # compares 0.25% versus 1% chitosan-genipin formulations; † compares 1% versus 1% chitosan-genipin formulations ($p < 0.05$, Student's t test).

Figure 6. Microcapsule protection and release of NCs in GI conditions. A) Nonencapsulated ^{125}I-IgG NCs versus ^{125}I-IgG NCs encapsulated in microcapsules were incubated for 2 h at 37 °C in SGF (pH 1.2) containing or not pepsin. Due to lack of NC release at this pH, microcapsules were dissolved in EDTA to examine the NC content. Degradation was assessed by quantifying free ^{125}Iodine, expressed as a percentage of the total radioisotope content. B) Microcapsules were incubated in SGF containing pepsin as in (A), followed by a 4 h incubation at 37 °C in SIF containing pancreatin (pH 7.8). The percentage of ^{125}I-IgG NCs released from microcapsules was determined by radioisotope tracing. Data are Mean ± S.E.M. * Compares nonencapsulated NCs versus other formulations; no statistically significant difference was observed between other groups ($p < 0.05$, one-way ANOVA followed by Tukey test). † Compares presence versus absence of pepsin; # compares 3 h versus 6 h ($p < 0.05$, Student's t test).

formulations (<15% degradation; Figure 6A). This was also the case for microcapsules containing IgG PLGA NCs, where the presence of pepsin did not increase the degree of degradation of the encapsulated NCs (Figure S5A, Supporting Information). Although having a similar pattern, in the absence of a chitosan
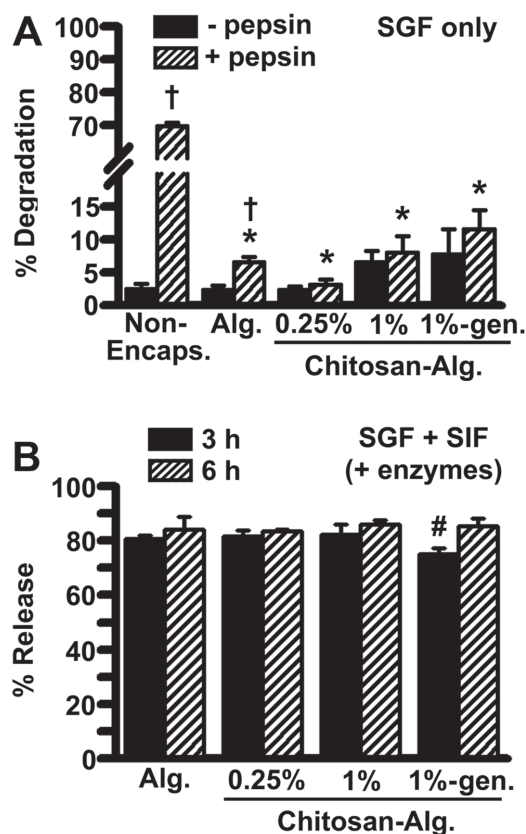
shell alginate microcapsules showed statistically lower protection (Figure 6A).

Then, we examined NC release after a 2 h incubation in pepsin-containing SGF, followed by a 4 h incubation in pancreatin-containing SIF (Figure 6B). Significant release (75%–80%) of encapsulated NCs occurred by 1 h in enzyme-containing SIF (Figure 6B), similar to previously observed in the absence of enzymes. Also, in the presence of GI enzymes a similar release behavior was found for antibody-coated PLGA NCs as compared to these model polystyrene counterparts (Figure S5B, Supporting Information). Hence, encapsulation within alginate and, primarily, chitosan–alginate microcapsules, prevents premature gastric degradation of the antibody counterpart while providing release in intestinal conditions.

2.7. Receptor Targeting by NCs Released from Microcapsules under GI Conditions

We then examined if antibody-coated NCs can bind an immobilized target (secondary antibody) when released from microcapsules after incubation in enzyme-containing SGF and SIF. To provide a baseline, we dissolved with EDTA microcapsules that had not been exposed to GI conditions and measured binding of the released NCs. NCs displayed substantial binding, 10^6–10^7 NCs per well, in the range of the binding provided by control NCs that had never been encapsulated (Figure S6, Supporting Information). Incubation of nonencapsulated NCs in gastric conditions (enzyme-containing SGF) followed or not by intestinal conditions (enzyme-containing SIF), resulted in a massive reduction in their binding ability: 10^2 NCs/well in SGF alone (95% reduced binding compared with storage conditions) and no detectable binding in SGF followed by SIF (**Figure 7**A). This parallels the high degradation observed for nonencapsulated counterparts (Figure 6A). In contrast, NCs encapsulated within microcapsules retained targeting ability: 10^5–10^7 NCs bound/well (Figure 7A). This suggests that the protection afforded by encapsulation may render sufficient receptor-targeting of antibody-coated NCs when administered via the oral route.

To further verify this hypothesis, we examined the targeting potential of anti-ICAM-coated NCs to ICAM-1 expressed on cells, after release from microcapsules. Since no major differences had been observed among the three chitosan–alginate formulations tested, we selected the simplest formulation composed of 0.25% chitosan–alginate to compare with alginate alone. As shown in Figure 7B, after 2 h in pepsin-containing SGF, minimal binding (eight NCs bound/cell) was observed for control anti-ICAM NCs that had never been encapsulated, as expected due to degradation (Figure 6A). In contrast, anti-ICAM NCs retained within microcapsules and then released by EDTA (since there is no release in SGF) revealed significant binding: 48 NCs/cell and 159 NCs/cell for alginate and chitosan–alginate formulations, respectively. This targeting was specific since control IgG NCs only resulted in four NCs bound/cell (49-fold below the level of anti-ICAM NC binding). Transfer of microcapsules from pepsin-containing SGF to pancreatin-containing SIF caused a reduction in anti-ICAM NC binding on cells (≈60% reduction), yet considerable binding was still detected: 60–70 NCs/cell. Hence, it may be possible to achieve receptor-mediated targeting of NCs via the oral route when encapsulated within protective microcapsules.

2.8. Oral Gavage of Encapsulated ICAM-1-Targeted Nanocarriers in Mice

Finally, we examined the degradation and biodistribution of encapsulated anti-ICAM NCs following in vivo administration in mice. For these studies, ^{125}I-anti-ICAM NCs were encapsulated in 0.25% chitosan–alginate microcapsules, which were administered to mice via oral gavage and compared to nonencapsulated ^{125}I-anti-ICAM NCs. We first evaluated whether microcapsules conferred protection against anti-ICAM degradation by quantifying the level of free ^{125}Iodine with respect to the total ^{125}Iodine content in each section of the GI tract
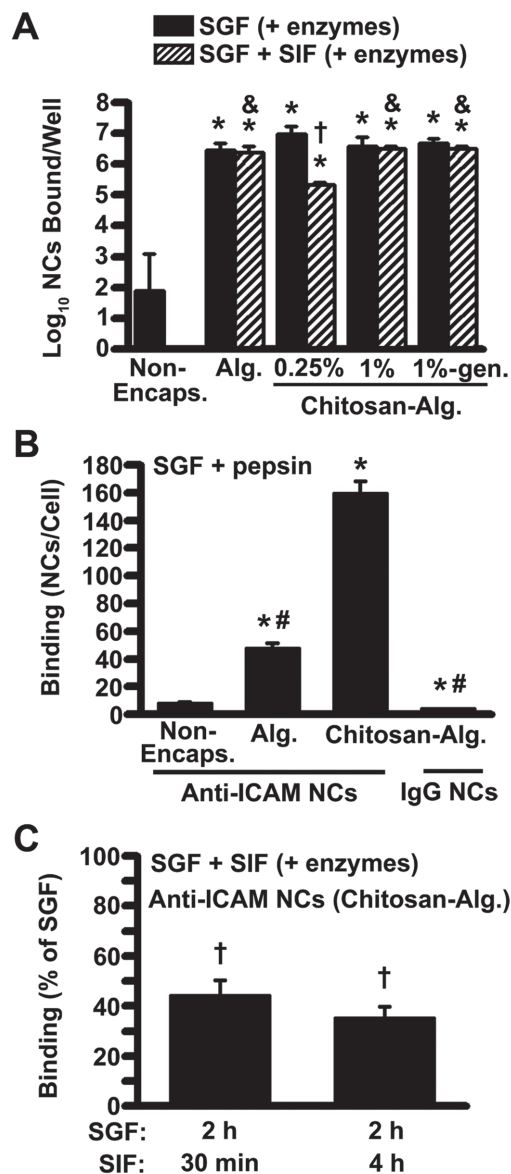

Figure 7. Receptor targeting by NCs released from microcapsules in GI conditions. Nonencapsulated ^{125}I-IgG NCs versus ^{125}I-IgG NCs in microcapsules were incubated in SGF or SGF followed by SIF (with enzymes). NCs released by EDTA after SGF incubation, or those naturally released after SGF + SIF incubation, were tested. A) Binding of nonencapsulated versus microcapsule-released ^{125}I-IgG NCs to secondary antibody-coated wells, measured by radioisotope tracing. B) Anti-ICAM NCs (nonencapsulated vs loaded in alginate or 0.25% chitosan–alginate microcapsules) versus nonspecific IgG NCs (loaded in 0.25% chitosan–alginate microcapsules) were incubated in pepsin-containing SGF as in (A). NCs were released by EDTA and binding was assessed by incubation for 2 h with ICAM-1-expressing cells. The number of NCs per cell was quantified by fluorescence microscopy. C) Cell binding of nonencapsulated versus anti-ICAM NCs released from microcapsules after gastric + intestinal conditions was examined by microscopy and normalized to binding prior to release in intestinal conditions. Data are Mean ± S.E.M. * Compares nonencapsulated versus encapsulated NCs; # compares to anti-ICAM NCs released from chitosan–alginate microcapsules; † compares SGF versus SGF followed by SIF; (p < 0.05, Student's *t* test). & Compares 0.25% chitosan versus other formulations (p < 0.05, one-way ANOVA followed by Tukey test).
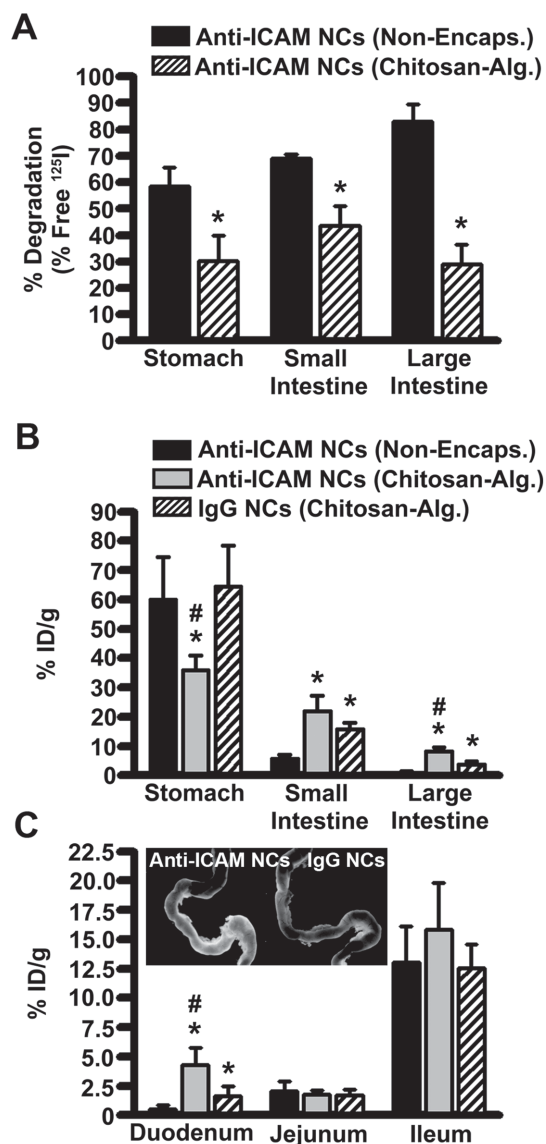
Materials Views
www.MaterialsViews.com

ADVANCED
FUNCTIONAL
MATERIALS
www.afm-journal.de

FULL PAPER

Figure 8. Protection and biodistribution of encapsulated ICAM-1-targeting NCs in the GI tract of mice. Mice were orally gavaged with ^{125}I-anti-ICAM NCs (nonencapsulated vs encapsulated in 0.25% chitosan–alginate microcapsules) or nonspecific ^{125}I-IgG NCs encapsulated in 0.25% chitosan–alginate microcapsules. 1 h after administration, the indicated sections of the GI tract were harvested to determine: A) the percentage of free ^{125}Iodine (reflective of degradation) with respect to the total ^{125}Iodine content, and B,C) the ^{125}I-content and tissue weight, to calculate the percent injected dose per gram (% ID/g). Data are Mean ± S.E.M. * Compares nonencapsulated and encapsulated groups. # compares encapsulated anti-ICAM NCs versus encapsulated IgG NCs. ($p < 0.05$, Student's t test). The inset in (C) shows the fluorescence visualization of the duodenal section of the GI for anti-ICAM NCs (left) versus IgG NCs (right).

(**Figure 8**A). In agreement with in vitro observations, encapsulation in chitosan–alginate microcapsules resulted in significant protection, with 60%–70% of the total antibody content being preserved, while only 20%–40% of the nonencapsulated control was preserved (approximately threefold enhanced protection). Importantly, anti-ICAM NC encapsulation within

microcapsules rendered lower retention in the stomach versus nonencapsulated counterparts (36% vs 59% ID/g), which is important for avoiding degradation (Figure 8B). Instead, encapsulation enhanced NC biodistribution in the small intestine (22% vs 6% ID/g) and the large intestine (8% vs 0.9% ID/g; Figure 8B), desirable for treatment of pathologies in these regions or absorption into the circulation. Additional examination showed that this enhanced intestinal biodistribution was attributed to ninefold greater localization in the duodenum. This is likely due to specific targeting of epithelial cells by anti-ICAM NCs.

Then, to assess targeting specificity, we compared anti-ICAM NCs to IgG NCs, both of which were encapsulated within 0.25% chitosan–alginate microcapsules. Similar to targeted counterparts, IgG NCs showed enhanced accumulation in the small and large intestine (16% and 4% ID/g) with respect to the nonencapsulated control (Figure 8B). However, intestinal accumulation was reduced compared to anti-ICAM NCs, suggesting specific targeting. In fact, duodenal biodistribution of IgG NCs was significantly lower (threefold) than anti-ICAM NCs, as measured using radioisotope tracing of the antibody coat (Figure 8C) and also imaged using fluorescent visualization of the NC counterpart (Figure 8C, inset; Figure S7, Supporting Information). Taken together, ICAM-1-targeted NCs encapsulated in chitosan–alginate microcapsules provide enhanced protection in the stomach, and site-specific accumulation in the small intestine, specifically the duodenum.

3. Discussion

Active targeting of drug carriers offers an opportunity to enhance drug biodistribution and transport within or across cells.[1–3] These advantages also apply to oral drug delivery.[5–12] However, most targeting moieties suffer inactivation or degradation en route to the intestine, an important target for therapeutic intervention and a primary site of drug absorption into the blood.[12] Although protective encapsulation of drugs, biologicals, etc. has been well studied,[21–35] this approach remains largely unexplored in the case of receptor-targeting NCs. Using the example of ICAM-1 targeting by model antibody-coated NCs, we have examined whether encapsulation in biopolymer-based microcapsules provides protection against degradation in gastric conditions, while allowing release and targeting under intestinal conditions.

We selected alginate microcapsules as a model based on its biocompatibility and gentle formulation.[23–32,49] The method employed produced uniform microcapsules in terms of geometry, with a suitable size for oral gavage in mice. The encapsulation efficiency was very high, with minimal release over 28 d in storage conditions. These parameters did not vary when alginate microcapsules were modified with chitosan shells, as expected since this modification was conducted after NC encapsulation into the alginate core. Comparison with literature data suggests that although these microcapsules may not prevent leaching of small molecules (≈1 nm in size),[22,23,26] they hereby prevented diffusion of encapsulated NCs. Also, while compromised capsule stability has been observed for loads that occupy a large volume within the capsule (e.g., mammalian cells),[27]

ADVANCED
FUNCTIONAL
MATERIALS
www.afm-journal.de

Materials
Views
www.MaterialsViews.com

FULL PAPER

this was not the case when NCs were used as a load in our study. Hence, NC encapsulation may be a viable application for biopolymer microcapsules. In fact, we observed minimal degradation of the antibody counterpart of NCs when incorporated within microcapsules, and encapsulated NCs retained ≈90% of their targeting ability. These results are key in pursuing receptor-targeting applications via oral delivery, and agree with reports documenting the binding ability of naked antibodies following encapsulation in chitosan–alginate.[26]

A prevailing requirement of encapsulation of oral therapies containing labile agents, such as targeting antibodies, is to provide protection from the gastric acidic pH and proteases.[21] In agreement with the literature, our alginate microcapsules remained insoluble and retained encapsulated NCs at gastric pH. The microcapsules also shrank in gastric buffer, which may result from the high osmotic concentrations in this medium.[23] The chitosan shell seemed permeable to ion exchange, as all chitosan–alginate formulations shrank similarly to alginate.

As expected, all microcapsules dissolved within 1 h of incubation at intestinal pH, likely due to Ca^{2+} displacement by monovalent ions under these conditions. Coating with 0.25% chitosan slightly reduced burst release, confirming previous reports.[25,26] While the alginate core dissolved, the chitosan shell allowed some microcapsules to remain visible. These "visible" microcapsules showed significant swelling, also in agreement with Ca^{2+} displacement by monovalent ions, suggested above. Importantly, the microcapsules retained the majority of the fluorescent content (the NC counterpart) by 1 h in intestinal pH, which was then slowly released by 4 h. Radioisotope tracing of the antibody counterpart revealed faster release, suggesting that some antibodies may detach from the NCs and diffuse through the chitosan shell. Yet, binding of released NCs to cells showed that sufficient antibodies remained on NCs as to provide targeting.

As said, swelling seemed to dictate the release from chitosan–alginate microcapsules. Increasing the concentration of chitosan from 0.25% to 1% did not significantly alter the degree of release, while genipin crosslinking curtailed the initial burst release, as in previous works.[36,48] All the microcapsules exhibited pH-sensitive release, which holds significance for oral formulations requiring protection from gastric conditions and release in intestinal conditions. In fact, in agreement with minimal release from microcapsules at gastric pH, encapsulated NCs showed minimal degradation and considerable targeting ability after microcapsule exposure to SGF with gastric enzymes. Nonencapsulated NCs were degraded to a much greater extent and showed little binding after incubation in this condition. Hence, the pore size of microcapsules seemed small enough as to prevent enzyme penetration into the alginate core. In addition, significant targeting was verified upon release in SIF with pancreatin, while binding of nonencapsulated counterparts was not possible in this condition. Therefore, encapsulation offers protection of targeted NCs in gastric and intestinal conditions with enzymes, preserving functionality of targeting moieties. Importantly, a similar pattern of gastric protection and intestinal release was observed for antibody-coated NCs consisting either of polystyrene or PLGA nanoparticles, emphasizing the relevance of this approach in future design of clinically relevant formulations.

An application that could benefit from this encapsulation strategy is targeting to ICAM-1. ICAM-1 is expressed on the GI and other tissues and is involved in GI pathologies associated with inflammation, including infections, immune alterations, cancers, genetic conditions, etc.[13,14] ICAM-1-targeting NCs and conjugates have shown promising results regarding delivery of therapeutic and imaging agents in numerous diseases.[37,38,40–45,50–60] Moreover, in GI epithelial monolayers, anti-ICAM NCs facilitated intra and transepithelial delivery of a model therapeutic enzyme (α-Galactosidase, deficient in Fabry disease[61]), revealing particular promise for oral delivery.[18] However, oral delivery in vivo was limited by premature degradation of anti-ICAM in the stomach.[20] Our results hereby indicate that encapsulation in chitosan–alginate microcapsules may help overcome these obstacles. In fact, after incubation in GI-like buffers with digestive enzymes, NCs released from microcapsules significantly and specifically bound to ICAM-1-expressing cells. Relative to nonencapsulated counterparts, microcapsules protected anti-ICAM NCs against degradation in all GI sections upon oral gavage in mice. Encapsulation lowered stomach retention and enhanced intestinal biodistribution, specifically in the duodenum, in agreement with the protection and release observed in vitro.

4. Conclusion

Alginate and chitosan–alginate microcapsules provided protection of antibody-targeted NCs in storage and gastric conditions, while allowing NCs release under intestinal conditions. Following transit through the gastric and intestinal milieus, NCs released from microcapsules retained significant targeting ability, measured in vitro, cell culture, and mice. Therefore, this encapsulation strategy may help implement oral delivery of targeted drug carriers. Whereas this concept was hereby illustrated for ICAM-1 targeting and antibody-coated polymer NCs, similar approaches may benefit other targeted systems which employ labile targeting moieties against this and other GI surface markers.

5. Experimental Section

Reagents: Mouse monoclonal IgG against human ICAM-1 (clone R6.5) and rat monoclonal IgG against mouse ICAM-1 (clone YN1), herein collectively called anti-ICAM, were isolated from the respective hybridomas from ATCC (Manassas, VA, USA). Mouse IgG, rat IgG, and goat anti-mouse IgG were from Jackson Immunoresearch (West Grove, PA, USA). Green Fluoresbrite® 100 nm diameter polystyrene particles were from Polysciences (Warrington, PA, USA). PLGA carboxylic-acid terminated (50:50 copolymer ratio; 32 kDa average molecular weight) was from Lakeshore Biomaterials (Birmingham, AL). Medium molecular weight chitosan (200–800 cps; 75%–85% deacetylated), alginic acid sodium salt from brown algae (low viscosity), fluorescein isothiocyanate isomer I (FITC), acetone, pepsin, and pancreatin were purchased from Sigma-Aldrich (St. Louis, MO, USA). Protease inhibitor cocktail was from Thermo Scientific (Rockford, IL, USA). SGF without enzymes and SIF without enzymes were from Cole-Parmer (Vernon-Hills, IL).

Preparation of Antibody-Coated NCs: Commercial green fluorescent (Fluoresbrite®) polystyrene nanoparticles (100 nm diameter) served as main model for an NC, as in Muro and co-workers.[18,19] Additionally,

www.MaterialsViews.com

ADVANCED
FUNCTIONAL
MATERIALS
www.afm-journal.de

FULL PAPER

key results were validated using PLGA counterparts. PLGA NCs were prepared using the nanoprecipitation with solvent evaporation method.[38] Briefly, an organic phase consisting of 475 mg of PLGA (50:50 copolymer ratio; 32 kDa average molecular weight) and 25 mg of FITC in 25 mL of acetone, was added under vigorous agitation into a surfactant-free aqueous phase consisting of 200 mL of filtered deionized water. The emulsion was stirred overnight at room temperature to allow evaporation of the organic solvent. The resulting nanoparticle suspension was filtered and dialyzed, and finally concentrated using a rotary evaporator.

Both types of nanoparticles were coated by surface adsorption with either IgG (IgG NCs) or anti-ICAM (anti-ICAM NCs), as described.[18,38] Where indicated, antibodies were labeled with ^{125}Iodine for quantification using a gamma-radiation counter (Wizard²; PerkinElmer). As described,[44,62] 5×10^{-6} M antibody was incubated with ≈10^{13} particles mL^{-1} to allow antibody adsorption on the particle. Noncoated antibody was removed by centrifugation at 13 800 × g for 3 min, and coated particles were resuspended at ≈7×10^{11} NCs mL^{-1} in 1% bovine serum albumin (BSA)-supplemented phosphate buffered saline (PBS), and sonicated to remove aggregates.[44,62] The diameter of the antibody-coated NCs was determined by nanoparticle tracking analysis (NanoSight LM10, Malvern Instruments, Westborough, MA), and the polydispersity index and ζ-potential by dynamic light scattering (Zetasizer NanoZS90, Malvern Instruments, Westborough, MA, USA). Since the number of particles in polystyrene standards was known, radioisotope quantification allowed us to calculate the number of antibodies per particle.[44,62] The resulting NCs are described in the Results.

Preparation of Microcapsules Containing Antibody-Coated NCs: Sodium alginate (3% w/v aqueous) was vortexed with antibody-coated NCs (16% v/v NCs to alginate; 2.7×10^{11} NCs g^{-1} alginate) and this solution was converted into uniform microdroplets using a flow of air described by Raghavan and co-workers.[47] The solution was pumped at 5 μL min^{-1} by a peristaltic syringe pump through capillary tubing (100 μm inner diameter) and a 5 psi co-axial air flow was used to generate droplets. Typical droplets produced under these conditions were ≈180 μm in diameter, which were dropped into a crosslinking medium of 2% CaCl$_2$ without stirring. This resulted in microcapsules with a gelled core of alginate chains crosslinked by Ca^{2+} ions. To create chitosan–alginate microcapsules, chitosan was dissolved in 1% v/v aqueous acetic acid at a concentration of 0.25 or 1% w/v, and adjusted to pH 5 using NaOH. The alginate microcapsules were incubated with this chitosan solution under gentle agitation, generating a chitosan shell. When indicated, rhodamine-labeled chitosan[46] (a gift from Dr. Payne, University of Maryland) was used to confirm the shell by fluorescence microscopy. To further stabilize the shell, an aqueous solution of 1 mg mL^{-1} genipin (an aglycone that crosslinks chitosan amine groups)[36] was incubated with 1% chitosan–alginate microcapsules.

Characterization of the NC Loading in the Microcapsules: Radioisotope quantification of ^{125}I-antibody-coated NCs was used to calculate the number of NCs per microcapsule, percent (%) loading, and EE%, as it follows:

$$NCs \ per \ microcapsule = CPM_{microcapsule}/CPM_{NC}$$

$$\%Loading = (NCs \ per \ microcapsule/NC \ Concentration)/V_{microcapsule} \times 100\%$$

$$EE\% = (Measured \ NCs \ per \ microcapsule/Added \ NCs \ per \ microcapsule) \times 100\%$$

where CPM are the ^{125}Iodine counts-per-minute per microcapsule (CPM$_{microcapsule}$) or per NC (CPM$_{NC}$), and V is the theoretical volume of each microcapsule (V$_{microcapsule}$), as derived from their mean diameter. In parallel with radioisotope tracing, fluorescence microscopy was used to verify the presence of NCs within microcapsule.

Microcapsule Stability and Release in Storage Conditions: To evaluate stability in storage, microcapsules loaded with antibody-coated, fluorescent NCs were incubated in 2% CaCl$_2$ at 4 °C for 28 d. At the indicated times, fluorescence microscopy was used to image sample aliquots, from which the size and number of visible microcapsules were quantified, along with their sum and mean fluorescence intensities. These parameters reflect microcapsule size, degradation, and loading over time, which were compared to day 1. Release of ^{125}I-antibody-coated, fluorescent NCs from the microcapsules was also quantified, using centrifugation at 1000 × g for 1 min to separate the released (supernatant) and encapsulated (pellet) fractions. The radioisotope (^{125}I-antibody coat) and fluorescence content (NC counterpart) of each fraction were quantified in a gamma counter and a spectrofluorometer, respectively. The percent release (from the total released + encapsulated content) was calculated.

Status of Microcapsule-Encapsulated NCs in Storage Conditions: Since no significant release of NCs from microcapsules was observed in storage, microcapsules were incubated in 50×10^{-3} M EDTA with shaking (150 rpm) to extract Ca^{2+} from the alginate matrix. The degradation of the ^{125}I-antibody moiety of encapsulated NCs was examined by quantifying free ^{125}Iodine in the released NC fraction after trichloroacetic acid precipitation.[45,62] This was expressed as a percentage of the total ^{125}Iodine content in the released fraction. In parallel, the ability of released NCs to bind to a surface-immobilized target (a secondary antibody) was evaluated. Wells were coated with 1 μg mL^{-1} goat anti-mouse IgG, washed and blocked with 1% BSA-PBS, and incubated for 16 h with antibody-coated NCs released from microcapsules. NCs that bound to the immobilized antibody and nonbound NCs were collected and measured in a gamma counter. The percentage of NCs bound from the total NCs added to wells and the absolute number of NCs bound per well were calculated. Antibody-coated NCs that had never been encapsulated within microcapsules were used as controls.

Microcapsule Stability and Release in Simulated Gastrointestinal Fluids: The stability of microcapsules loaded with antibody-coated NCs and the release of this content from microcapsules were evaluated using radiotracing and fluorescence microscopy, as above. Conditions mimicking the physiological pH of the GI were used, adopted from U.S. Pharmacopeia (USP). Briefly, NC-loaded microcapsules were first incubated for 2 h at 37 °C in SGF (pH 1.2), then transferred to SIF (pH 6.8) for 4 h at 37 °C, always under agitation (150 rpm). Aliquots from the SGF and SIF solutions were taken at the indicated times to evaluate the microcapsule size, number of microcapsules that appeared visibly intact, fluorescence loading, and ^{125}I-antibody.

Status of Encapsulated and Released NCs in Simulated Gastrointestinal Conditions: Microcapsules were incubated for 2 h at 37 °C in SGF with or without pepsin, then analyzed or transferred to SIF with or without pancreatin for 4 h at 37 °C. Since microcapsules incubated in SGF showed no release, antibody-coated NCs were collected by dissolving microcapsules with EDTA. This step was not necessary upon incubation in SIF, since NC were released in this condition. Degradation of antibodies from the NC coat was assessed by quantifying free ^{125}Iodine content versus total ^{125}Iodine content of the released NC fraction, as described above. The ability of the released NCs to bind a surface-immobilized target (secondary antibody) was assessed as above. The percentage of NCs bound with respect to the total NCs added to wells and the absolute number of NCs bound per well were calculated. Antibody-coated NCs that had never been encapsulated within microcapsules were used as controls.

Specific Cell Targeting of Antibody-Coated NCs after Release from Microcapsules: Fluorescent IgG NCs or anti-ICAM NCs were encapsulated in alginate microcapsules or 0.25% chitosan–alginate microcapsules. The microcapsules were then incubated in SGF with pepsin followed by SIF with pancreatin, as described above. At the indicated times, NCs released from microcapsules were incubated for 2 h with cells known to express ICAM-1 (see below). Samples were imaged by fluorescence microscopy to quantify the number of NCs bound per cell, using algorithms previously described.[15,44,62] Binding was compared to that of anti-ICAM NCs that had been never encapsulated but subjected to the same GI-mimicking conditions.

Human umbilical vein endothelial cells (HUVECs; Clonetics; San Diego, CA, USA) were used, where targeting of anti-ICAM NCs has been tested previously.[15–17,62] HUVECs were grown at 37 °C in M199

FULL PAPER

medium (GibcoBRL, Grand Island, NY, USA) supplemented with 15% fetal bovine serum, 2×10^{-3} M glutamine, 15 mg mL^{-1} endothelial cell growth supplement, 100 mg mL^{-1} heparin, and antibiotics. Cells were seeded onto gelatin-coated coverslips and treated for 16 h with 10 ng mL^{-1} tumor necrosis factor-alpha (BD Biosciences, Franklin Lakes, NJ, USA) to induce ICAM-1 expression.[13,14] Fixed (2% paraformaldehyde) samples were used.

Microscopy Visualization and Image Analysis: PlanApo objectives and the Olympus IX81 inverted 3-axe automatic fluorescence microscope (Olympus Inc., Center Valley, PA) were used. Samples were observed by phase contrast and fluorescence using green and red filters from Semrock (Rochester, NY). Micrographs were taken using Orca-ER camera from Hamamatsu (Bridgewater, NJ) and SlideBook 4.2 software from Intelligent Imaging Innovations (Denver, CO). Images were analyzed using Image-Pro 6.3 from Media Cybernetics Inc. (Bethesda, MD) to quantify microcapsule diameter, sum fluorescence per microcapsule (equivalent to fluorescent NC content), mean fluorescence per microcapsule (sum fluorescence per area, equivalent to the distribution of NC content), and number of NCs per cell.

Oral Gavage in Mice: C57BL/6 mice (Jackson Laboratory, Bar Harbor, ME) were fasted for 2–4 h.[20] Then, mice underwent oral gavage with 0.25% chitosan–alginate microcapsules ($\approx 1.5 \times 10^4$ microcapsules/animal) loaded with ^{125}I-anti-ICAM NCs or ^{125}I-IgG NCs, versus nonencapsulated ^{125}I-anti-ICAM NCs. Doses were ≈ 1.1 mg antibody kg^{-1} body weight (as measured using a gamma counter), equivalent to 1.5×10^{13} NCs kg^{-1} (calculated from the specific radioactivity of NCs). After 1 h from oral gavage, mice were sacrificed and the stomach, small intestine (duodenum, jejunum, and ileum), and large intestine (cecum and colon) were isolated. ^{125}Iodine, percent free ^{125}Iodine, and the weight were measured.[20,62] These data were used to calculate percentage of injected dose per gram (% ID/g) in GI compartments, and the degradation of the antibody (labile) counterpart of NCs.[20] Alternatively, the GI tracts of mice gavaged with green fluorescent, nonradioactive anti-ICAM NCs, or IgG NCs were fixed in 4% paraformaldehyde and imaged in a Bi-O-Vision TVD1000R UV transilluminator (Spectroline; Spectronics Corporation, Westbury, NY). Studies were approved by IACUC and the University of Maryland regulations.

Statistical Analysis: Data were calculated as mean ± standard error of the mean (S.E.M). For in vitro and animal studies the number of independent samples was ≥6, and for cell assays the number of independent wells was ≥4. Statistical significance was determined by Student's unpaired *t*-tests for comparisons between two groups, and one-way ANOVA followed by Tukey test for comparisons among more than two groups. Differences were considered significant at p < 0.05.

Supporting Information

Supporting Information is available from the Wiley Online Library or from the author.

Acknowledgements

[1] L. Rajendran, H. J. Knolker, K. Simons, *Nat. Rev. Drug Discov.* **2010**, *9*, 29.

[2] R. Duncan, S. C. Richardson, *Mol. Pharm.* **2012**, *9*, 2380.

[3] S. Muro, *J. Controlled Release* **2012**, *164*, 125.

[4] V. Torchilin, *Eur. J. Pharm. Biopharm.* **2009**, *71*, 431.

[5] J. H. Hamman, P. H. Demana, E. I. Olivier, *Drug Target Insights* **2007**, *2*, 71.

[6] V. K. Pawar, J. G. Meher, Y. Singh, M. Chaurasia, B. Surendar Reddy, M. K. Chourasia, *J. Controlled Release* **2014**, *196*, 168.

[7] K. B. Chalasani, G. J. Russell-Jones, A. K. Jain, P. V. Diwan, S. K. Jain, *J. Controlled Release* **2007**, *122*, 141.

[8] H. H. Salman, C. Gamazo, P. C. de Smidt, G. Russell-Jones, J. M. Irache, *Pharm. Res.* **2008**, *25*, 2859.

[9] S. Jain, V. V. Rathi, A. K. Jain, M. Das, C. Godugu, *Nanomedicine* **2012**, *7*, 1311.

[10] V. Fievez, L. Plapied, A. des Rieux, V. Pourcelle, H. Freichels, V. Wascotte, M. L. Vanderhaeghen, C. Jerome, A. Vanderplasschen, J. Marchand-Brynaert, Y. J. Schneider, V. Preat, *Eur. J. Pharm. Biopharm.* **2009**, *73*, 16.

[11] P. N. Gupta, K. Khatri, A. K. Goyal, N. Mishra, S. P. Vyas, *J. Drug Target* **2007**, *15*, 701.

[12] Y. Yun, Y. W. Cho, K. Park, *Adv. Drug Delivery Rev.* **2013**, *65*, 822.

[13] S. Muro, in *Endothelial Biomedicine* (Ed: W. C. Aird), Cambridge University Press, New York **2007**, p. 1058.

[14] D. Serrano, S. Muro, in *Mechanobiology of the Endothelium* (Ed: H. Aranda-Espinoza), CRC Press, Boca Raton **2015**, p. 185.

[15] S. Muro, R. Wiewrodt, A. Thomas, L. Koniaris, S. M. Albelda, V. R. Muzykantov, M. Koval, *J. Cell Sci.* **2003**, *116*, 1599.

[16] D. Serrano, T. Bhowmick, R. Chadha, C. Garnacho, S. Muro, *Arterioscler., Thromb., Vasc. Biol.* **2012**, *32*, 1178.

[17] C. Garnacho, D. Serrano, S. Muro, *J. Pharmacol. Exp. Ther.* **2012**, *340*, 638.

[18] R. Ghaffarian, T. Bhowmick, S. Muro, *J. Controlled Release* **2012**, *163*, 25.

[19] J. Hsu, J. Rappaport, S. Muro, *Pharm. Res.* **2014**, *31*, 1855.

[20] V. Mane, S. Muro, *Int. J. Nanomed.* **2012**, *7*, 4223.

[21] L. A. Sharpe, A. M. Daily, S. D. Horava, N. Peppas, *Expert Opin. Drug Delivery* **2014**, *11*, 901.

[22] M. George, T. E. Abraham, *J. Controlled Release* **2006**, *114*, 1.

[23] K. Y. Lee, D. J. Mooney, *Prog. Polym. Sci.* **2012**, *37*, 106.

[24] F. Goycoolea, G. Lollo, C. Remuñán-Lopez, F. Quaglia, M. J. Alonso, *Biomacromolecules* **2009**, *10*, 1736.

[25] A. K. Anal, D. Bhopatkar, S. Tokura, H. Tamura, W. F. Stevens, *Drug Dev. Ind. Pharm.* **2003**, *29*, 713.

[26] X. Y. Li, L. J. Jin, Y. N. Lu, Y. H. Zhen, S. Y. Li, L. H. Wang, Y. P. Xu, *Appl. Biochem. Biotechnol.* **2009**, *159*, 778.

[27] S. Sugiura, T. Oda, Y. Aoyagi, R. Matsuo, T. Enomoto, K. Matsumoto, T. Nakamura, M. Satake, A. Ochiai, N. Ohkohchi, M. Nakajima, *Biomed. Microdevices* **2007**, *9*, 91.

[28] S. Takka, A. Gurel, *AAPS PharmSciTech* **2010**, *11*, 460.

[29] H. Onishi, K. Koyama, O. Sakata, Y. Machida, *Drug Dev. Ind. Pharm.* **2010**, *36*, 879.

[30] G. D'Orazio, P. Di Gennaro, M. Boccarusso, I. Presti, G. Bizzaro, S. Giardina, A. Michelotti, V. Labra, B. La Ferla, *Appl. Microbiol. Biotechnol.* **2015**, *22*, 9779.

[31] T. Jiang, B. Singh, S. Maharjan, H. S. Li, S. K. Kang, J. D. Bok, C. S. Cho, Y. J. Choi, *Eur. J. Pharm. Biopharm.* **2014**, *88*, 768.

[32] Y. Zhang, W. Wei, P. Lv, L. Wang, G. Ma, *Eur. J. Pharm. Biopharm.* **2011**, *77*, 11.

[33] M. B. Dowling, A. S. Bagal, S. R. Raghavan, *Langmuir* **2013**, *29*, 7993.

[34] A. Trapani, A. Lopedota, M. Franco, N. Cioffi, E. Ieva, M. Garcia-Fuentes, M. J. Alonso, *Eur. J. Pharm. Biopharm.* **2010**, *75*, 26.

www.MaterialsViews.com

ADVANCED
FUNCTIONAL
MATERIALS
www.afm-journal.de

FULL PAPER

[35] J. Y. Hou, L. N. Gao, F. Y. Meng, Y. L. Cui, *Marine Drugs* **2014**, *12*, 5764.

[36] H. Chen, W. Ouyang, C. Martoni, S. Prakash, *Int. J. Polym. Sci.* **2009**, *3643*, 1.

[37] C. Garnacho, R. Dhami, E. Simone, T. Dziubla, J. Leferovich, E. H. Schuchman, V. Muzykantov, S. Muro, *J. Pharmacol. Exp. Ther.* **2008**, *325*, 400.

[38] S. Muro, T. Dziubla, W. Qiu, J. Leferovich, X. Cui, E. Berk, V. R. Muzykantov, *J. Pharmacol. Exp. Ther.* **2006**, *317*, 1161.

[39] M. Wiseman, C. W. Frank, *Langmuir* **2012**, *28*, 1765.

[40] R. Ghaffarian, S. Muro, *Mol. Pharm.* **2014**, *11*, 4350.

[41] A. J. Calderon, V. Muzykantov, S. Muro, D. M. Eckmann, *Biorheology* **2009**, *46*, 323.

[42] T. Bhowmick, E. Berk, X. Cui, V. R. Muzykantov, S. Muro, *J. Controlled Release* **2012**, *157*, 485.

[43] J. Papademetriou, C. Garnacho, D. Serrano, T. Bhowmick, E. H. Schuchman, S. Muro, *J. Inherited Metab. Dis.* **2013**, *36*, 467.

[44] J. Hsu, L. Northrup, T. Bhowmick, S. Muro, *Nanomedicine* **2012**, *8*, 731.

[45] J. Hsu, D. Serrano, T. Bhowmick, K. Kumar, Y. Shen, Y. C. Kuo, C. Garnacho, S. Muro, *J. Controlled Release* **2011**, *149*, 323.

[46] Y. Cheng, X. Luo, J. Betz, S. Buckhout-White, O. Bekdash, G. F. Payne, W. E. Bentley, G. W. Rubloff, *Soft Matter* **2010**, *6*, 3177.

[47] A. X. Lu, *Ph.D. Thesis*, University of Maryland (College Park) **2015**.

[48] B. Manickam, R. Sreedharan, M. Elumalai, *Curr. Drug Deliv.* **2014**, *11*, 139.

[49] S. Sugiura, T. Oda, Y. Izumida, Y. Aoyagi, M. Satake, A. Ochiai, N. Ohkohchi, M. Nakajima, *Biomaterials* **2005**, *26*, 3327.

[50] J. Papademetriou, Z. Tsinas, J. Hsu, S. Muro, *J. Controlled Release* **2014**, *188*, 87.

[51] S. Muro, *Adv. Funct. Mater.* **2014**, *24*, 2899.

[52] A. J. Hamilton, S. L. Huang, D. Warnick, M. Rabbat, B. Kane, A. Nagaraj, M. Klegerman, D. D. McPherson, *J. Am. Coll. Cardiol.* **2004**, *43*, 453.

[53] G. E. Weller, F. S. Villanueva, E. M. Tom, W. R. Wagner, *Biotechnol. Bioeng.* **2005**, *92*, 780.

[54] S. Park, S. Kang, A. J. Veach, Y. Vedvyas, R. Zarnegar, J. Y. Kim, M. M. Jin, *Biomaterials* **2010**, *31*, 7766.

[55] J. C. Murciano, S. Muro, L. Koniaris, M. Christofidou-Solomidou, D. W. Harshaw, S. M. Albelda, D. N. Granger, D. B. Cines, V. R. Muzykantov, *Blood* **2003**, *101*, 3977.

[56] B. Zern, A. M. Chacko, J. Liu, C. F. Greineder, E. R. Blankemeyer, R. Radhakrishnan, V. Muzykantov, *ACS Nano* **2013**, *7*, 2461.

[57] C. Chittasupho, S. X. Xie, A. Baoum, T. Yakovleva, T. J. Siahaan, C. J. Berkland, *Eur. J. Pharm. Sci.* **2009**, *37*, 141.

[58] A. C. Anselmo, S. Kumar, V. Gupta, A. M. Pearce, A. Ragusa, V. Muzykantov, S. Mitragotri, *Biomaterials* **2015**, *68*, 1.

[59] M. F. Kiani, H. Yuan, X. Chen, L. Smith, M. W. Gaber, D. J. Goetz, *Pharm. Res.* **2002**, *19*, 1317.

[60] P. Guo, J. Huang, L. Wang, D. Jia, J. Yang, D. A. Dillon, D. Zurakowski, H. Mao, M. A. Moses, D. T. Auguste, *Proc. Natl. Acad. Sci. USA* **2014**, *111*, 14710.

[61] R. J. Desnik, E. H. Schuchman, *Ann. Rev. Genomics Hum. Genet.* **2012**, *13*, 307.

[62] S. Muro, V. R Muzykantov, J. Murciano, in *Bioconjugation Protocols* (Ed. C. M. Niemeyer), Humana Press, New Jersey, USA **2004**, p. 21.

ADVANCED
FUNCTIONAL
MATERIALS

Supporting Information

Chitosan–Alginate Microcapsules Provide Gastric Protection and Intestinal Release of ICAM-1-Targeting Nanocarriers, Enabling GI Targeting In Vivo

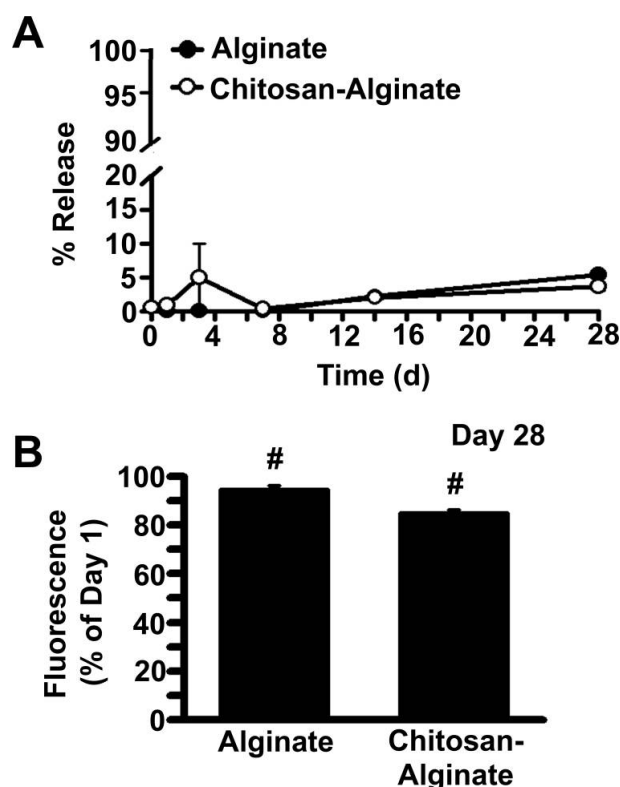*Rasa Ghaffarian, Edgar Pérez-Herrero, Hyuntaek Oh, Srinivasa R. Raghavan, and Silvia Muro**

Supporting Information

Chitosan-Alginate Microcapsules Provide Gastric Protection and Intestinal Release of ICAM-1-Targeting Nanocarriers, Enabling GI Targeting In Vivo

Rasa Ghaffarian, Edgar Pérez-Herrero, Hyuntaek Oh, Srinivasa R. Raghavan, and Silvia Muro*

Figure S1. Release of fluorescent NCs from microspheres in storage conditions. Alginate vs. 0.25% chitosan-alginate microspheres containing IgG-coated fluorescent NCs were incubated in storage conditions as in Fig. 3. (A) At the indicated times, aliquots were removed to assess the fluorescent NC content in the released vs. encapsulated fractions by spectrofluorometry. (B) At day 28 in storage conditions, the sum fluorescence (in A.U.) per microsphere was quantified by microscopy and expressed as a percentage of the fluorescence measured at day 1. Data are Mean ± S.E.M. No statistically significant differences were observed between alginate and chitosan-alginate formulations. # Compares values at day 28 vs. day 1 ($p<0.05$, Student's t test).
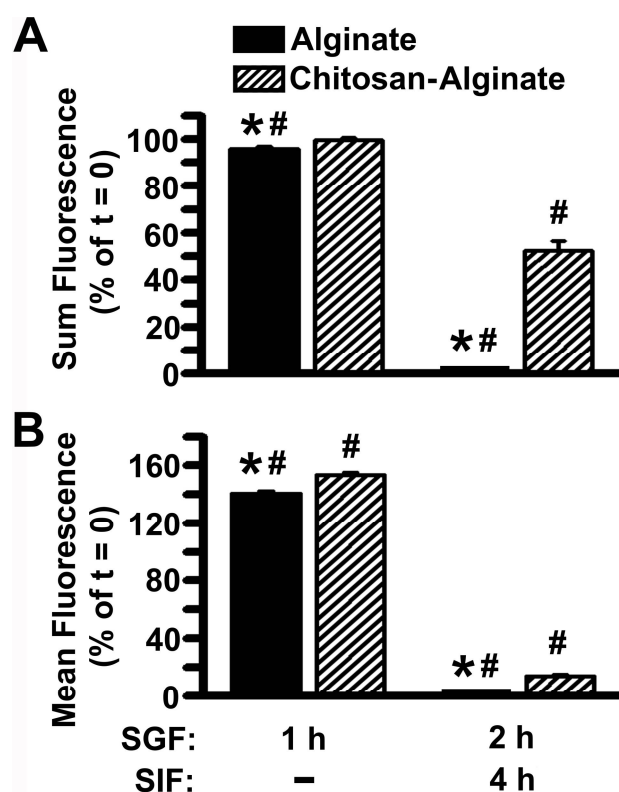
Figure S2. pH-dependent release of fluorescent NCs from microspheres. Alginate and 0.25% chitosan-alginate microspheres loaded with IgG-coated fluorescent NCs were incubated for 2 h in SGF (pH 1.2) followed by a 4 h incubation in SIF (pH 7.8), as described in Fig. 4. At the indicated times, the (A) sum fluorescence and (B) mean fluorescence intensity (sum / area) of visibly intact microspheres were quantified from microscopy images. Values were expressed as a percentage of those measured prior to incubations (t = 0). Data are Mean ± S.E.M. * Compares alginate vs. chitosan-alginate formulations; # compares each time point against t = 0 (p<0.05, Student's *t* test).

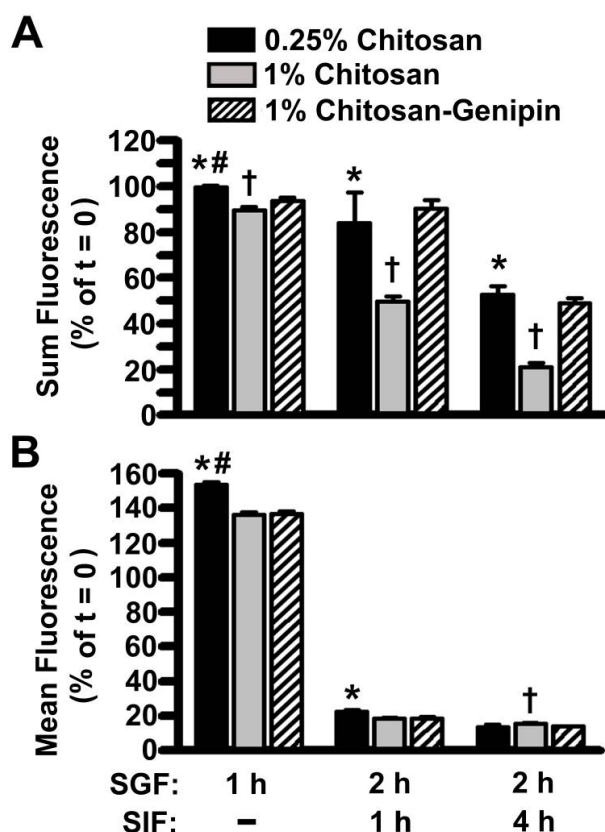**Figure S3. Effect of chitosan concentration and crosslinking on the pH-dependent release of fluorescent NCs.** Alginate microspheres loaded with ^{125}I-IgG fluorescent NCs were coated with 0.25% chitosan, 1% chitosan, or genipin-crosslinked 1% chitosan, and incubated in for 2 h in SGF (pH 1.2) followed by 4 h in SIF (pH 7.8). At the indicated times, the (A) sum fluorescence and (B) mean fluorescence intensity (sum / area) of visibly intact microspheres were quantified from microscopy images. Values were expressed as the percentage of those measured prior to incubations (t = 0). Data are Mean ± S.E.M. * Compares 0.25% vs. 1% chitosan formulations; # compares 0.25% vs. 1% chitosan-genipin formulations; †, compares 1% vs. 1% chitosan-genipin formulations (p<0.05, Student's *t* test).

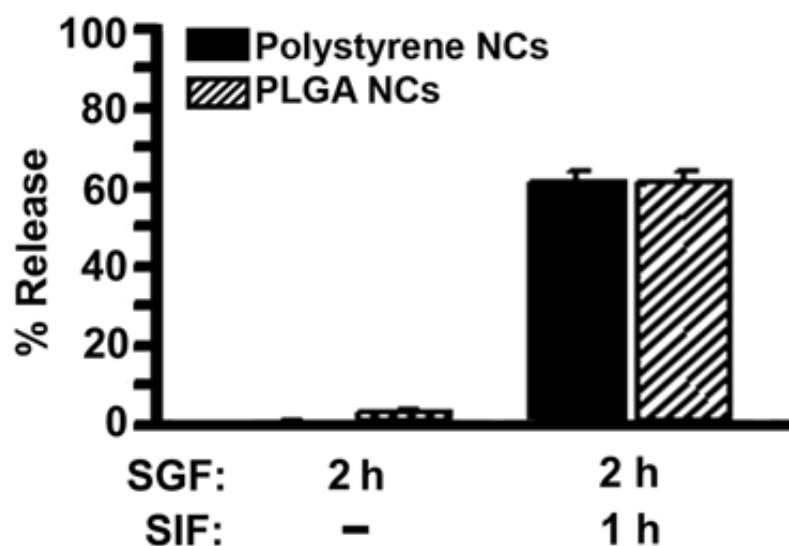**Figure S4. pH-dependent release of PLGA NCs from microcapsules** 1% chitosan-alginate microcapsules containing either ^{125}I-IgG-coated polystyrene NCs or ^{125}I-IgG-coated PLGA NCs were incubated for 2 h at 37 ˚C in SGF (pH 1.2) followed or not by 1 h in SIF (pH 7.8). At the indicated times, aliquots were removed to assess the release of encapsulated NCs using radioisotope tracing. Data are Mean ± S.E.M.
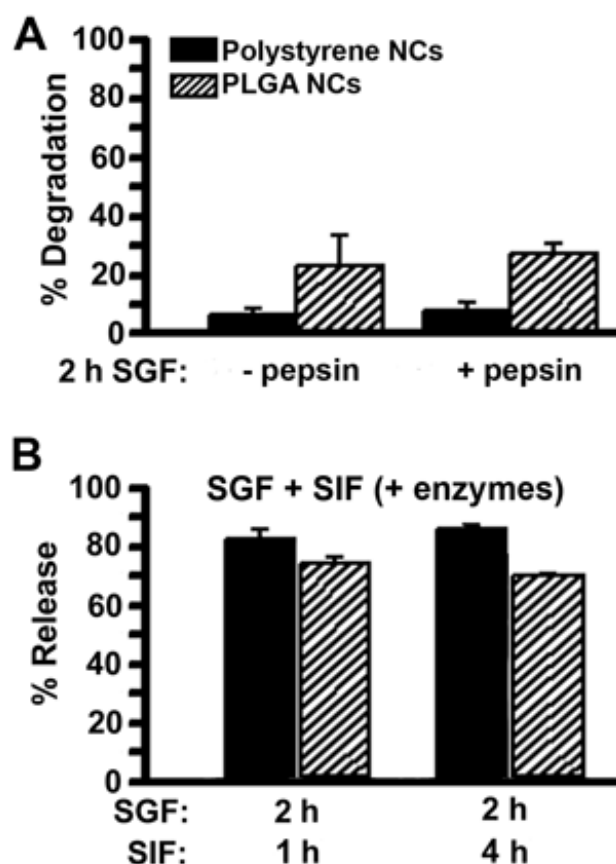
Figure S5. Microcapsule protection and release of PLGA NCs in GI conditions. (A) ^{125}I-IgG-coated polystyrene NCs or PLGA NCs were encapsulated in 1% chitosan-alginate microcapsules and then incubated for 2 h at 37 ˚C in SGF (pH 1.2) containing or not pepsin. Degradation was assessed by quantifying free [125]Iodine, expressed as a percentage of the total radioisotope content. (B) Microcapsules were incubated in SGF containing pepsin as in (A), followed by a either 1 h or 4 h incubation at 37 ˚C in SIF containing pancreatin (pH 7.8). The percentage of ^{125}I-IgG polystyrene or PLGS NCs released from microcapsules was determined by radioisotope tracing. Data are Mean ± S.E.M.
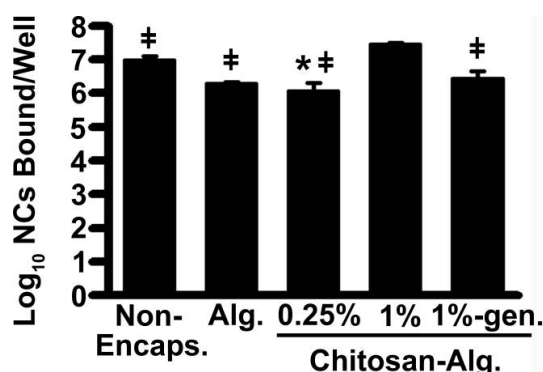
Figure S6. Binding of fluorescent NCs released from microspheres in GI conditions. The binding ability of non-encapsulated ^{125}I-IgG NCs vs. ^{125}I-IgG NCs encapsulated in alginate, 0.25% chitosan-, 1% chitosan-, or genipin-1% chitosan-alginate microspheres was assessed after 1 day in control storage conditions vs. binding of respective formulations in GI conditions. This required release of NCs by EDTA-induced dissolution of microspheres, since no natural release occurs in storage. IgG NCs were incubated with secondary antibody-coated wells to allow binding, as described in Fig. 3. Wells were washed to remove non-bound counterparts, and radioisotope tracing was used to quantify the number of NCs bound per well. Data are Mean ± S.E.M. * Compares non-encapsulated NCs vs. other formulations; ‡, compares 1% chitosan microspheres vs. other formulations ($p < 0.05$, one-way ANOVA followed by Tukey test).
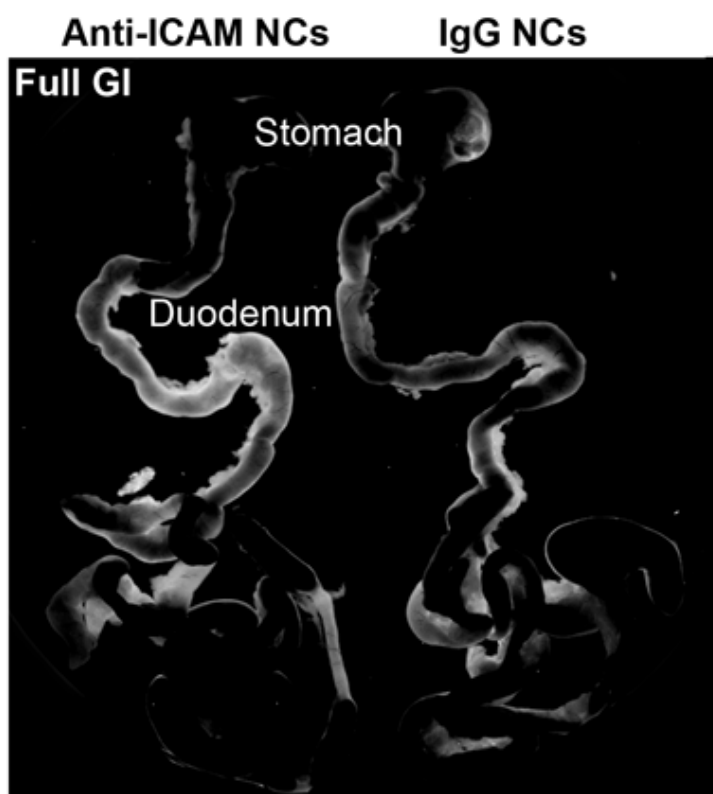
Figure S7. Visualization of antibody-coated NCs in the GI tract. Mice were gavaged with either anti-ICAM NCs or IgG NCs (green fluorescent, polystyrene models) and sacrificed 1 h later. Their GI tracts were then excised, fixed, and illuminated by UV light. Stomach and duodenal sections are indicated.